RSC Advances

PAPER

View Article Online
View Journal | View Issue

Cite this: *RSC Adv.*, 2016, **6**, 78311

Temperature-dependent photoluminescence of inorganic perovskite nanocrystal films

Jiaming Li,[ab] Xi Yuan,[b] Pengtao Jing,[c] Ji Li,[b] Maobin Wei,[b] Jie Hua,[b] Jialong Zhao*[b] and Lianhua Tian*[a]

Received 2nd July 2016
Accepted 10th August 2016

DOI: 10.1039/c6ra17008k

www.rsc.org/advances

Temperature-dependent photoluminescence (PL) properties of inorganic perovskite $CsPbBr_3$ nanocrystal (NC) films were studied by using steady-state and time-resolved PL spectroscopy. The closely packed solid films were obtained by dropping NC solution on silicon substrates. It was found that the PL intensities of the NC films, which are dependent on the size of NCs, slightly decreased with increasing temperature to 300 K, while the PL intensities dropped rapidly with increasing temperature above 300 K and were nearly quenched at 360 K. Further the corresponding average PL lifetimes increased significantly with increasing temperature below about 320 K and then significantly became shorter. The PL quenching mechanisms were demonstrated through heating and cooling experiments. The experimental results indicated inorganic perovskite NCs exhibited a thermal PL quenching in the temperature range of 80–300 K and a thermal degradation at temperatures above 300 K. The linewidths, peak energies, and lifetimes of PL emissions for the NC films as a function of temperature were discussed in detail.

Introduction

All-inorganic perovskite nanocrystals (NCs) have attracted much attention for applications in light emitting diodes (LEDs),[1–3] lasers,[4–6] and photodetectors.[7] In the 1990s, luminescent $CsPbX_3$ (X = Cl, Br) NCs with quantum size effects were successfully grown in CsCl and CsBr single crystals, respectively.[8] The broad emissions of $CsPbBr_3$ NCs were considered to come from the recombination of free or trapped excitons by using steady-state and time-resolved photoluminescence (PL) spectroscopy at various temperatures.[9–12] Recently highly luminescent colloidal $CsPbX_3$ (X = Cl, Br, I) NCs were synthesized using a high-temperature hot-injection approach and anion exchange reactions.[13–17] Compared with Cd-based core/shell quantum dots, these $CsPbX_3$ NCs without a semiconductor shell exhibit size- or composition-tunable emissions from 400 to 700 nm, narrow emission line widths of 10–40 nm, and high quantum yields of over 80%. In particular, $CsPbX_3$ NCs with nearly free mid-gap trap states are a good candidate for replacing the Cd-based quantum dots as light sources in the blue, green, and red spectral region. It is necessary to study the PL properties of these $CsPbX_3$ NCs for both fundamental researches and commercial applications.

The temperature-dependent PL spectroscopy has been widely used to study the nonradiative relaxation processes and exciton–phonon coupling in colloidal CdSe and PbS quantum dots.[18–20] In general, the integrated PL intensities of the colloidal CdSe and PbS quantum dots decrease with increasing temperature, which is due to thermal quenching. Usually the PL quenching will result in a decrease in PL lifetimes.[20,21] The thermal quenching behaviour is usually related to carrier trapping by large amount of surface states/traps or thermal escape of carriers assisted by the scattering with multiple longitudinal optical (LO) phonons. The temperature dependent PL spectra of $CsPbBr_3$ NCs in CsBr single crystals have been demonstrated the thermal quenching at temperature up to 200 K.[9–11] However, so far no report has been given about the thermal stability of PL emissions in colloidal inorganic perovskite NCs with different size.

In this work we report a study on the temperature dependent PL spectra of colloidal $CsPbBr_3$ NC films using steady-state and time-resolved PL spectroscopy. The PL intensities, peak energies, linewidths, and lifetimes of the NCs as a function of temperature are studied systematically. The thermal stability and quenching mechanisms of PL emissions for the NCs with various sizes are discussed.

Experimental section

$CsPbBr_3$ were synthesized with a hot-injection approach.[13–15] For $CsPbBr_3$ NCs, $PbBr_2$ and octadecene were loaded into a 50 mL 3-

[a]*Department of Physics, College of Science, Yanbian University, Yanji 133002, China. E-mail: lhtian@ybu.edu.cn*

[b]*Key Laboratory of Functional Materials Physics and Chemistry of the Ministry of Education, Jilin Normal University, Siping 136000, China. E-mail: zhaojl@ciomp.ac.cn*

[c]*State Key Laboratory of Luminescence and Applications, Changchun Institute of Optics, Fine Mechanics and Physics, Chinese Academy of Sciences, Changchun 130033, China*

neck flask, degassed at 120 °C for 30 min. Oleylamine and oleic acid were injected at 120 °C under N_2. After complete solubilisation of a $PbBr_2$ salt, the temperature was heated to 160 °C and Cs-oleate solution obtained by dissolving $CsCO_3$ in octadecene and oleic acid at 150 °C was quickly injected. After 5 seconds, the reaction mixture was cooled by the ice-water bath. The closely packed solid films for X-ray diffraction (XRD) and temperature-dependent PL measurements were fabricated *via* dropping NC solution on silicon substrates.

The absorption spectrum measurements were performed on a UV-vis spectrophotometer (Shimadzu UV-2700). The PL emission spectra, decay curves, and quantum yields were obtained using a spectrometer (Horiba Jobin Yvon Fluorolog-3) with a time-correlated single-photon counting spectrometer and a quantum yield accessory. The morphologies of the $CsPbBr_3$ NCs were characterized by a transmission electron microscope (TEM, JEOL JEM2100) operated at 200 kV. The XRD patterns were recorded using a Rigaku D/max-2500 diffractometer with Cu Kα radiation at room temperature. The temperature-dependent PL measurements were performed using a vacuum liquid nitrogen cryostat (Janis VPF-500) with a temperature controller.

Results and discussion

Fig. 1 shows the absorption and PL emission spectra of $CsPbBr_3$ NCs in hexane. The absorption bands of $CsPbBr_3$ NCs are very broad at room temperature due to size distribution of NCs or thermal ionization of excitons in NCs. $CsPbBr_3$ NCs (NC493) exhibit a clear absorption peak except NC512 and NC516 samples. The exciton absorption bands of these NCs were estimated to be 478, 499, and 506 nm, respectively. The smaller $CsPbBr_3$ NCs have a broad emission peak at 493 nm with a full width at half maximum (FWHM) of 23.5 nm (119.5 meV), the medium ones have a narrow emission peak at 512 nm with an FWHM of only 16.5 nm (78.1 meV), and the largest ones exhibit a narrow emission peak at 516 nm with an FWHM of only 17 nm (78.9 meV). The PL spectral properties of the NCs are similar to those reported recently in literature.[13–17] Three NC samples above are labelled as NC493, NC512 and NC516, respectively. The small Stokes shifts of 15.4 nm (81.0 meV) for NC493, 13.8 nm (67.0 meV) for NC512 and 10.1 nm (47.5 meV) for NC516 indicate that the PL emissions of these NCs may originate from the radiative recombination of free excitons or bound excitons. Further the $CsPbBr_3$ NC films on Si substrates exhibit a PL peak at 496, 514, and 518 nm with FWHMs of 22.7 nm (114.6 meV), 16.5 nm (77.1 meV), and 18.5 nm (85.4 meV) for NC493, NC512, and NC516 samples, respectively, which slightly red-shifted, compared to that of the corresponding NCs in hexane. The red shifts of emission peaks in the NC films are probably related to the energy transfer from small NCs to large ones.[22,23] The absolute PL quantum yields of above 70% for diluted NC solutions were determined using a fluorescence spectrometer with an integrated sphere excited at a wavelength of 450 nm. The high PL quantum yields indicate the low nonradiative recombination in colloidal $CsPbBr_3$ NCs.

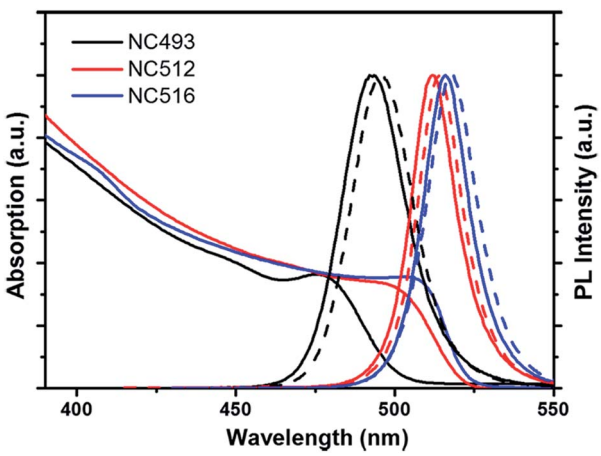

Fig. 1 Absorption (solid lines, left) and PL (solid lines, right) spectra of $CsPbBr_3$ NCs with emissions of 493, 512 nm, and 516 nm. The black, red, and blue dashed lines represent the PL spectra of the NCs in solid films, respectively. The PL emission spectra are normalized for comparison. Excitation wavelength is 405 nm.

Typical TEM images and XRD patterns of $CsPbBr_3$ NCs are shown in Fig. 2. As seen in Fig. 2a–c, the NCs are cubes in shape. The $CsPbBr_3$ NCs for NC493 have an average cube length of 6.14 nm with a size deviation of 0.98 nm, while the NCs for NC512 exhibit an average cube length of 9.39 nm with a size deviation of 1.14 nm. The $CsPbBr_3$ NCs for NC516 possess an average cube length of 12.1 nm with a size deviation of 2.37 nm. Further, the observation of lattice spacing in the HRTEM image of a NC for NC512 as shown in Fig. 2d clearly indicates the good crystallinity of the synthesized NCs. The XRD patterns of $CsPbBr_3$ (NC493, NC512, and NC516) NC films are shown in Fig. 2e. It can be seen that three samples exhibit a cubic perovskite structure (JCPDS no. 54-0752). Only the (100) and (200) diffraction peaks of the cubic perovskite structure are observed, which indicates that NC solid films have (100) preferred orientation. The crystallite sizes and lattice constants calculated from the XRD data are 6.6, 9.0, 10.8 nm and 0.5934, 0.5873, 0.5834 nm, respectively, based on the position and width of (200) diffraction peak using MDI Jade 6.5 software. The difference in size of $CsPbBr_3$ NCs for NC516 estimated by TEM and XRD is probably understood due to size distribution of NCs. In addition, the lattice spacing of about 0.59 nm for $CsPbBr_3$ NCs obtained from TEM and XRD is consistent with the previous result.[24] On the other hand, the blue shift of $CsPbBr_3$ NCs observed in their absorption peak and PL band with the decrease of size can be understood as follows. The absorption band is considered to originate from the exciton in NCs while the PL emission is probably from the many recombination channels.

The energies were obtained to be 2.62, 2.46, and 2.41 eV with sizes of 6.14, 9.39 and 12.0 nm, in good agreement with the energies of exciton absorption peaks at 2.59, 2.48, and 2.45 eV for NC493, NC 512 and NC 516, respectively. Therefore, our experimental results are consistent with the theoretical calculation.[13]

Fig. 3 shows the PL spectra of closely packed $CsPbBr_3$ NC films for NC493, NC512, and NC516 samples at temperatures

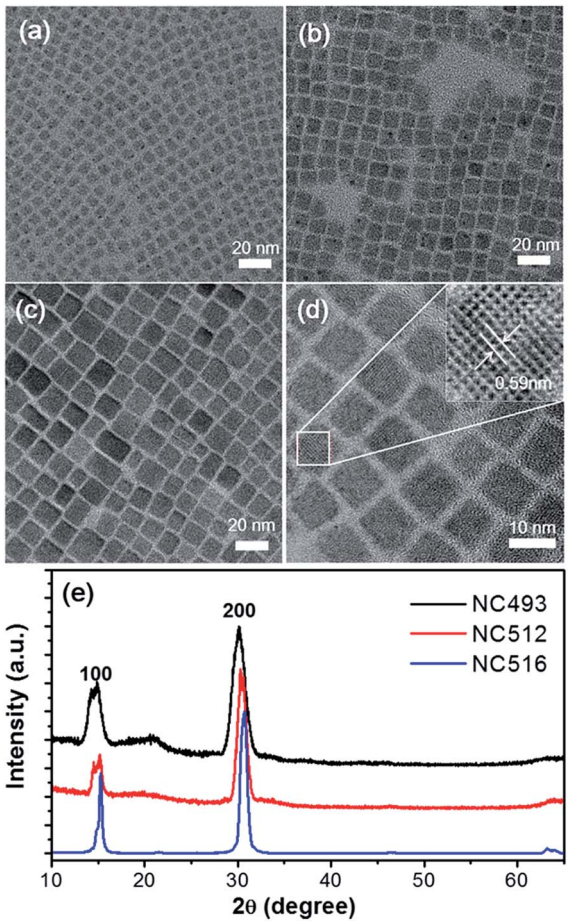

Fig. 2 Typical TEM images of inorganic perovskite NC films for NC493 (a), NC512 (b), and NC516 (c), the high resolution TEM image for NC512 (d), and their XRD patterns (e).

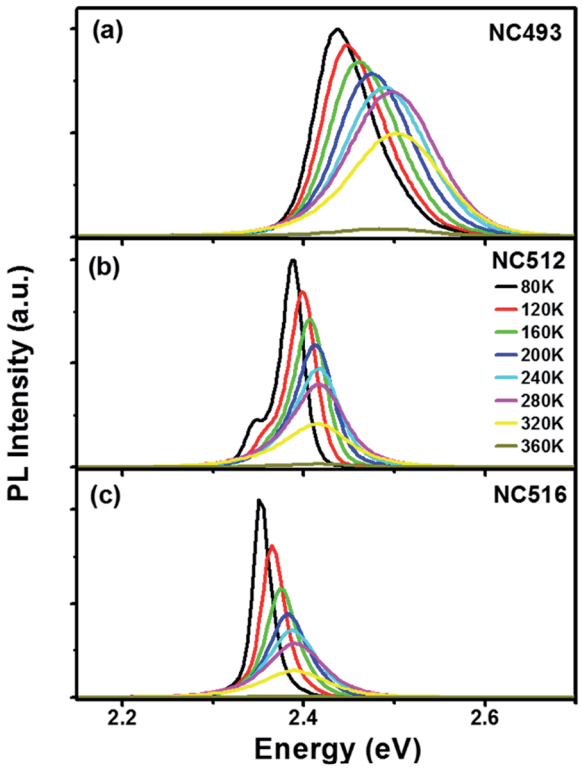

Fig. 3 Temperature-dependent PL spectra of $CsPbBr_3$ NC films for NC493 (a), NC512 (b), and NC516 (c) in the temperature range of 80–360 K.

ranging from 80 K to 360 K. The PL intensities are normalized at the maximum intensity to clarify the change of emission intensities and the shift of emission peaks for various samples. The variation in the PL spectra of the NC films was examined under excitation wavelength of 405 nm. As seen in Fig. 3, these NC films exhibit a decrease in the PL intensity with increasing temperature. Besides the peak energies of these NC films shift to higher energy side and the PL emission linewidths significantly increase with increasing the temperature. It is noted that the PL spectra of the NCs at 80 K are not symmetrical due to size distribution.[25] In addition, a small side peak of the PL at 2.3488 eV was observed in NC 512 sample. The energy spacing of the small peak with the large peak is 38.5 meV, which is larger than the phonon energy of about 20 meV obtained in this work as shown in Fig. 4. This means that the small peak of PL in NC512 is not from a phonon sideband. The small peak of PL might originate from the defects in the NCs.[10,11] The PL intensities, peak energies, and linewidths of $CsPbBr_3$ NC films at temperatures ranging from 80 K to 360 K are shown in Fig. 4.

As seen in Fig. 4a, the integrated PL intensities for NC493, NC512, and NC516 samples slightly decreases with increasing the temperature to 300 K, indicating thermal quenching of PL emission. The PL intensities as a function of temperature were fitted as shown in Fig. 4a by using the Arrhenius equation: $I(T) = I_0/(1 + A\exp(E_A/k_BT))$, in which I_0 is the intensity at 80 K, E_A is the activation energy, and k_B is the Boltzmann constant. The activation energy was obtained to be 54.7 meV for NC493, 43.4 meV for NC512, and 35.0 meV for NC516, respectively. It is found that the activation energy of $CsPbBr_3$ NCs increases with decreasing the size of NCs. The activation energy can be considered to be exciton binding energy if no other non-radiative decay channel is in the recombination process of exciton in the organic–inorganic hybrid perovskite NCs.[26,27] The high PL QY (~70%) of these $CsPbBr_3$ NCs confirms negligible defects or traps. Therefore, the $CsPbBr_3$ NCs have increased exciton binding energy with the decrease of size, resulting in more stable PL than the single crystals of $CsPbBr_3$ with exciton binding energy of 35.0 meV.[28,29] With further increase of temperature above 300 K the PL intensities of the $CsPbBr_3$ NCs drop rapidly. In contrast, the variation in PL intensity of organometal halide perovskite quantum dot films is not significant in the temperature range of 300–400 K.[26,27]

For common CdSe and InP quantum dots, they have a red shift in absorption band gap and PL band with increasing temperature. The temperature dependence of band gap can be described by the Varshni equation.[18–20] However, for PbS and PbSe quantum dots, they exhibit a blue shift of band gap and PL emission when the temperature is increased. The inorganic perovskite NCs exhibit a significant blue shift in band gap and

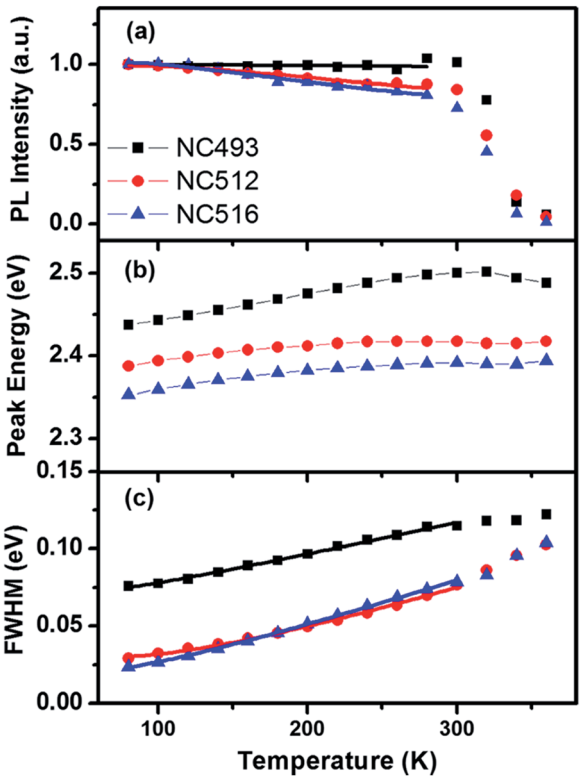

Fig. 4 PL intensities (a), peak energies (b), and linewidths (c) of $CsPbBr_3$ NC films as a function of temperature. The solid lines in (a) and (c) represent the fitting curves. The dashed lines in (b) are guided to eyes.

PL emission with increasing temperature, which is quite similar to the PbS and PbSe quantum dots. The blue shift is considered to originate from the electron–phonon coupling. The peak energies of emissions of the NC films for NC493, NC512, and NC516 are determined to be 2.44, 2.39, and 2.35 eV at 80 K and 2.50, 2.42, and 2.39 eV at 300 K, respectively, as seen in Fig. 4b. The smallest $CsPbBr_3$ NCs for NC493 have a significant blue shift in peak energy (0.27 meV K^{-1}) while the medium and largest $CsPbBr_3$ NCs for NC512 and NC516 show a weak blue shift, which is 0.18 and 0.17 meV K^{-1} in the temperature range of 80–300 K, respectively. The blue shifts in our NC samples with increasing temperature are smaller than those (about 0.5 meV K^{-1}) of in $CsPbBr_3$ NCs in CsBr and $CsPbBr_3$ crystals and 0.35 meV K^{-1} of $CsPbBr_3$ nanowires.[9,11,28,30] In particular, no significant shift in PL emissions of the NCs is observed at temperature above 300 K as shown in Fig. 4b, which is in agreement with that of $CsPbBr_3$ NCs reported recently.[16] On the other hand, the exciton–phonon coupling of the NCs in solid films was studied by measuring the temperature dependence of the PL linewidth broadening. The significant broadening in linewidths for the inorganic perovskite NC films for NC493, NC512, and NC516 is observed in Fig. 4c due to exciton–phonon coupling. The temperature-dependent linewidth of PL emissions for the NCs is described by the expression: $\Gamma(T) = \Gamma_0 + \Gamma_{op} \exp(\hbar\omega_{op}/k_BT - 1)$. Here the first term, Γ_0, is the inhomogeneous broadening contribution and Γ_{op} describes the interactions of exciton–optical phonon contributions to the linewidth broadening. The LO phonon energies ($\hbar\omega_{op}$) of NC493, NC512, and NC527 samples were estimated to be 14.4, 33.3, and 26.7 meV, which are close to phonon energy of 20.5 meV, previously obtained using Raman spectroscopy[28] and a LO phonon energy of 16.0 meV, estimating from temperature-dependent PL spectra of $CsPbBr_3$ crystals.[31]

Fig. 5 shows the PL decay curves and lifetimes of $CsPbBr_3$ NC films in the temperature range from 80 K to 360 K. It is noted that the PL decays become longer with increasing temperature while the PL decays suddenly become shorter after the temperature reaches about 320–340 K for NC493, NC512 and NC516, respectively. These PL lifetimes for all the samples are reduced after temperature is increased to about 320–340 K, which is slightly lower than the temperature of about 300 K that PL intensities started to decrease at. The PL decay curves can be described by a triexponential function: $I(t) = A_1 \exp(-t/\tau_1) + A_2 \exp(-t/\tau_2) + A_3 \exp(-t/\tau_3)$. The average PL lifetimes can be obtained by an expression: $\tau_{av} = ((A_1 \times \tau_1^2) + (A_2 \times \tau_2^2) + (A_3 \times \tau_3^2))/((A_1 \times \tau_1) + (A_2 \times \tau_2) + (A_3 \times \tau_3))$. The triexponential decay behaviour may result from the size distribution or three different species involved in the emission, compared with that of single NC.[32] Therefore the average PL lifetimes of the NC films for NC493, NC512, and NC516 were determined to be 2.25, 1.50 and 1.67 ns at 80 K and 3.64, 8.81, and 8.71 ns at 300 K, respectively, which are comparable to the $CsPbBr_3$ NCs (average lifetime of 11.5 ns) and thin films (average lifetime of 3.9 ns).[3,33] The average PL lifetimes of $CsPbBr_3$ NC films as a function of temperature are shown in Fig. 5d. It is clearly seen that the average PL lifetimes of the NC films increase with increasing temperature below temperature of 320–340 K, and then significantly decrease. The decrease in PL intensities and lifetimes of the inorganic perovskite NCs with increasing temperature above 300 K might result from the thermal degradation of the NCs because the loss of ligands on the surface of NCs or formation of nonradiative recombination centers does not occur at the low temperature.[19] As seen in Fig. 5, the PL lifetimes for NC516 sample decrease at 320 K earlier than that of the

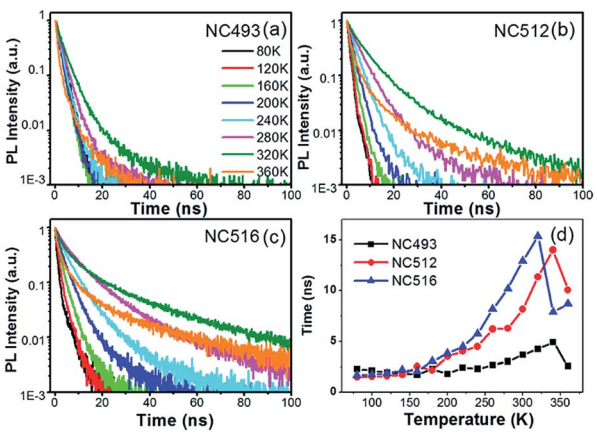

Fig. 5 PL decay curves of $CsPbBr_3$ NC films for NC493 (a), NC512 (b) and NC516 (c) samples and their average PL lifetimes (d) at various temperatures. The solid lines in (d) are guided to eyes.

other two samples perhaps due to the change of emission centers with relatively long PL lifetime. It has been observed that the phase transition of perovskite $CsPbCl_3$ resulted in a sharp decrease in PL intensity at temperature above 150 K.[34]

In general, the PL decays for one kind of emitters vary with their PL intensity, having the same temperature dependence. For most of colloidal quantum dots such as CdSe and PbS, both their PL intensities and lifetimes decrease with increasing temperature due to dominant emission from exciton recombination.[20,21] However, the lengthening of the average PL lifetimes has also been observed in the colloidal CdSe quantum dots recently, which was explained by introducing the charge carrier trapping at surface states or localized states as relaxation pathway and using a classical charge transfer theory.[35,36] More recently the photoactivation of $CsPbBr_3$ NCs and blinking of single dots have revealed the existence of the trap states in the NCs.[30,37] This may mean the existence of surface states or localized states in these perovskite NCs used in this experiment. Therefore, the PL emission of the NCs can tentatively be understood in terms of recombination of free excitons or localized excitons trapped at surface states,[3,33,38] having PL lifetimes in the range of 1–20 ns. The interaction of excitons with surface states with increasing temperature may results in an increase in PL lifetime of NCs.[35,36] At present the increase of PL lifetime in $CsPbBr_3$ NCs with the increase of temperature has not been understood completely. The similar trend was observed in organic–inorganic hybrid perovskite films.[39,40] In addition, it is also noted that the PL lifetime of the inorganic perovskite NCs with a longer emission wavelength becomes significantly long perhaps due to the increase in the density of surface states in NCs.

We have observed a rapid decrease in PL intensities of $CsPbBr_3$ NCs with further increase of temperature above 300 K as seen in Fig. 4a. To understand the thermal quenching behaviour of the NCs, the experiment of the heating and cooling processes in two temperature regions: 80–280 K (I) and 240–360 K (II) for NC493, NC512, and NC516 samples was carried out. Fig. 6 shows the temperature dependent PL intensities of $CsPbBr_3$ (NC516) NC films. It is found that the PL changes in region I could be fully reversible, which suggest the $CsPbBr_3$ NCs are stable in this temperature region. While, in the region II, up to 360 K, the PL thermal quenching can not be recovered, which may result from thermal degradation. This indicates that PL of core $CsPbBr_3$ NCs are not thermally stable above room temperature. The decrease in PL quantum yield of the colloidal quantum dots was related to the loss of ligands on the surface of dots.[19,41,42] Therefore thermal degradation of PL in the $CsPbBr_3$ NCs in this work is considered to result from the loss of ligands on the surface of NCs. In colloidal solution, the number of ligands on the surface of $CsPbBr_3$ NCs might keep a constant with increasing temperature so that the PL intensity of $CsPbBr_3$ NCs did not show a significant change in a previous report.[16]

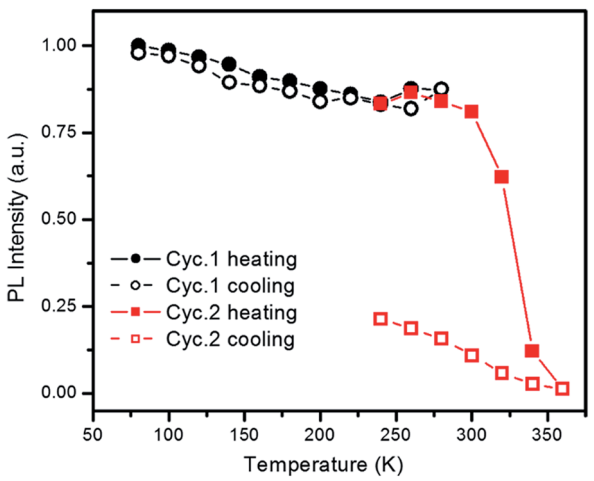

Fig. 6 Variation of temperature dependent PL intensity of $CsPbBr_3$ NC films. Circles mark the first thermal cycle (80–280 K), and squares represent the second cycle (240–360 K). The solid and open patterns refer to the heating and cooling processes for NC516.

Conclusions

In conclusion, we have studied the thermal stability of PL emissions from inorganic perovskite $CsPbBr_3$ NC films using steady-state and time-resolved PL spectroscopy. It was found that the PL intensities of the NCs in films slightly decreased with increasing temperature below 300 K, and then rapidly dropped to be nearly quenched at 360 K. The corresponding PL lifetimes increased significantly with increasing temperature to 320–340 K, and then significantly decreased for $CsPbBr_3$ NC films, respectively. The reversible and irreversible PL quenching mechanisms were demonstrated through heating and cooling experiments. Based on the temperature dependence of PL linewidths, peak energies and lifetimes, the PL emissions in $CsPbBr_3$ NCs were suggested to come from the recombination of excitons or localized excitons. Our experimental results indicated that these $CsPbBr_3$ NC films became unstable when temperature was higher than 300 K. Therefore, further works are needed to improve thermal stability of the all-inorganic perovskite NCs for applications in LEDs and lasers by modifying their surface properties and structures.

Acknowledgements

This work was supported by the National Natural Science Foundation of China (No. 11274304 and No. 21371071), Key Program for the Development of Science and Technology of Jilin Province (No. 20150204067GX), and the Thirteenth Five-Year Program for Science and Technology of Education Department of Jilin Province (No. 2016215). J. Z. thanks Dr Wenjin Zhang (Xingzi New Material Technology Development Co., Ltd.) for help of sample preparation.

Notes and references

1 J. Z. Song, J. H. Li, X. M. Li, L. M. Xu, Y. H. Dong and H. B. Zeng, *Adv. Mater.*, 2015, **27**, 7162–7167.
2 X. Y. Zhang, H. Lin, H. Huang, C. Reckmeier, Y. Zhang, W. C. H. Choy and A. L. Rogach, *Nano Lett.*, 2016, **16**, 1415–1420.

3 N. Yantara, S. Bhaumik, F. Yan, D. Sabba, H. A. Dewi, N. Mathews, P. P. Boix, H. V. Demir and S. Mhaisalkar, *J. Phys. Chem. Lett.*, 2015, **6**, 4360–4364.
4 Y. Wang, X. M. Li, X. Zhao, L. Xiao, H. Zeng and H. D. Sun, *Nano Lett.*, 2016, **16**, 448–453.
5 J. Pan, S. P. Sarmah, B. Murali, I. Dursun, W. Peng, M. R. Parida, J. Liu, L. Sinatra, N. Alyami, C. Zhao, E. Alarousu, T. K. Ng, B. S. Ooi, O. M. Bakr and O. F. Mohammed, *J. Phys. Chem. Lett.*, 2015, **6**, 5027–5033.
6 S. Yakunin, L. Protesescu, F. Krieg, M. I. Bodnarchuk, G. Nedelcu, M. Humer, G. D. Luca, M. Fiebig, W. Heiss and M. V. Kovalenko, *Nat. Commun.*, 2015, **6**, 8056.
7 P. Ramasamy, D. H. Lim, B. Kim, S. H. Lee, M. S. Lee and J. S. Lee, *Chem. Commun.*, 2016, **52**, 2067–2070.
8 M. Nikl, K. Nitsch, K. Polak, E. Mihokova, S. Zazubovich, G. P. Pazzi, P. Fabeni, L. Salvini, R. Aceves, M. Barbosa-Flores, R. P. Salas, M. Gurioli and A. Scacco, *J. Lumin.*, 1997, **72–74**, 377–379.
9 V. Babin, P. Fabeni, M. Nikl, G. P. Pazzi, I. Sildos, N. Zazubovich and S. Zazubovich, *Chem. Phys. Lett.*, 1999, **314**, 31–36.
10 M. Nikl, K. Nitsch, E. Mihokova, K. Polak, P. Fabeni, G. P. Pazzi, M. Gurioli, S. Santucci, R. Phani, A. Scacco and F. Somma, *Phys. E*, 1999, **4**, 323–331.
11 R. Aceves, V. Babin, M. Barboza Flores, P. Fabeni, A. Maaroos, M. Nikl, K. Nitsch, G. P. Pazzi, R. Perez Salas, I. Sildos, N. Zazubovich and S. Zazubovich, *J. Lumin.*, 2001, **93**, 27–41.
12 K. Nitsch, V. Hamplova, M. Nikl, K. Polak and M. Rodova, *Chem. Phys. Lett.*, 1996, **258**, 518–522.
13 L. Protesescu, S. Yakunin, M. I. Bodnarchuk, F. Krieg, R. Caputo, C. H. Hendon, R. X. Yang, A. Walsh and M. V. Kovalenko, *Nano Lett.*, 2015, **15**, 3692–3696.
14 G. Nedelcu, L. Protesescu, S. Yakunin, M. I. Bodnarchuk, M. J. Grotevent and M. V. Kovalenko, *Nano Lett.*, 2015, **15**, 5635–5640.
15 Q. A. Akkerman, V. D'Innocenzo, S. Accornero, A. Scarpellini, A. Petrozza, M. Prato and L. Manna, *J. Am. Chem. Soc.*, 2015, **137**, 10276–10281.
16 A. Swarnkar, R. Chulliyil, V. K. Ravi, M. Irfanullah, A. Chowdhury and A. Nag, *Angew. Chem., Int. Ed.*, 2015, **54**, 15424–15428.
17 I. Lignos, S. Stavrakis, G. Nedelcu, L. Protesescu, A. J. deMello and M. V. Kovalenko, *Nano Lett.*, 2016, **16**, 1869–1877.
18 P. T. Jing, J. J. Zheng, M. Ikezawa, X. Y. Liu, S. Z Lu, X. G. Kong, J. L. Zhao and Y. Masumoto, *J. Phys. Chem. C*, 2009, **113**, 13545–13550.
19 Y. Zhao, C. Riemersma, F. Pietra, R. Koole, C. de Mello Donega and A. Meijerink, *ACS Nano*, 2012, **6**, 9058–9067.
20 M. S. Gaponenko, A. A. Lutich, N. A. Tolstik, A. A. Onushchenko, A. M. Malyarevich, E. P. Petrov and K. V. Yumashev, *Phys. Rev. B: Condens. Matter Mater. Phys.*, 2010, **82**, 125320.
21 C. de Mello Donegá, M. Bode and A. Meijerink, *Phys. Rev. B: Condens. Matter Mater. Phys.*, 2006, **74**, 085320.
22 S. A. Crooker, J. A. Hollingsworth, S. Tretiak and V. I. Klimov, *Phys. Rev. Lett.*, 2002, **89**, 186802.
23 W. Lü, I. Kamiya, M. Ichida and H. Ando, *Appl. Phys. Lett.*, 2009, **95**, 083102.
24 C. K. Moller, *Nature*, 1958, **182**, 1436.
25 M. Koolyk, D. Amgar, S. Aharon and L. Etgar, *Nanoscale*, 2016, **8**, 6403–6409.
26 F. Zhang, H. Z. Zhong, C. Chen, X. G. Wu, X. M. Hu, H. L. Huang, J. B. Han, B. S. Zou and Y. P. Dong, *ACS Nano*, 2015, **9**, 4533–4542.
27 K. W. Wu, A. Bera, C. Ma, Y. M. Du, Y. Yang, L. Li and T. Wu, *Phys. Chem. Chem. Phys.*, 2014, **16**, 22476–22481.
28 C. C. Stoumpos, C. D. Malliakas, J. A. Peters, Z. Liu, M. Sebastian, J. Im, T. C. Chasapis, A. C. Wibowo, D. Y. Chung, A. J. Freeman, B. W. Wessels and M. G. Kanatzidis, *Cryst. Growth Des.*, 2013, **13**, 2722–2727.
29 D. Frohlich, K. Heidrich, H. Kunzel, G. Trendel and J. Treusch, *J. Lumin.*, 1979, **18/19**, 385–388.
30 D. D. Zhang, S. W. Eaton, Y. Yu, L. Dou and P. D. Yang, *J. Am. Chem. Soc.*, 2015, **137**, 9230–9233.
31 M. Sebastian, J. A. Peters, C. C. Stoumpos, J. Im, S. S. Kostina, Z. Liu, M. G. Kanatzidis, A. J. Freeman and B. W. Wessels, *Phys. Rev. B: Condens. Matter Mater. Phys.*, 2015, **92**, 235210.
32 F. R. Hu, H. C. Zhang, C. Sun, C. Y. Yin, B. H. Lv, C. F. Zhang, W. W. Yu, X. Y. Wang, Y. Zhang and M. Xiao, *ACS Nano*, 2015, **9**, 12410–12416.
33 S. B. Sun, D. Yuan, Y. Xu, A. F. Wang and Z. T. Deng, *ACS Nano*, 2016, **10**, 3648–3657.
34 T. Hayashi, T. Kobayashi, M. Iwanaga and M. Watanabe, *J. Lumin.*, 2001, **94–95**, 255–259.
35 M. Jones, S. S. Lo and G. D. Scholes, *Proc. Natl. Acad. Sci. U. S. A.*, 2009, **106**, 3011–3016.
36 M. Jones, S. S. Lo and G. D. Scholes, *J. Phys. Chem. C*, 2009, **113**, 18632–18642.
37 S. Seth, N. Mondal, S. Patra and A. Samanta, *J. Phys. Chem. Lett.*, 2016, **7**, 266–271.
38 J. A. Christians, J. S. Manser and P. V. Kamat, *J. Phys. Chem. Lett.*, 2015, **6**, 2086–2095.
39 C. Wehrenfennig, M. Z. Liu, H. J. Snaith, M. B. Johnston and L. M. Herza, *APL Mater.*, 2014, **2**, 081513.
40 H. H. Fang, F. Wang, S. Adjokatse, N. Zhao, J. Even and M. A. Loi, *Light: Sci. Appl.*, 2016, **5**, e16056.
41 X. Yuan, J. Zheng, R. Zeng, P. Jing, W. Ji, J. Zhao, W. Yang and H. Li, *Nanoscale*, 2014, **6**, 300–307.
42 J. M. Li, Y. Liu, J. Hua, L. H. Tian and J. L. Zhao, *RSC Adv.*, 2016, **6**, 44859–44864.

